

HIGH-GAIN FEL IN THE SPACE-CHARGE DOMINATED RAMAN LIMIT

I. Gadjev, C. Emma, A. Nause, J. Rosenzweig, UCLA, Los Angeles, USA

Abstract

While FEL technology has reached the EUV and X-ray regime at existing machines such as LCLS and SACLA, the scale of these projects is often impractical for research and industrial applications. Sub-millimeter period undulators can reduce the size of a high-gain EUV FEL, but will impose stringent conditions on the electron beam. In particular, a high-gain EUV FEL based on undulators with a sub-millimeter period [1] will require electron beam currents upwards of 1 kA at energies below 100 MeV. Coupled with the small gap of such undulators and their low undulator strengths, $K < 0.1$, these beam parameters bring longitudinal space-charge effects to the foreground of the FEL process. When the wavelength of plasma oscillations in the electron beam becomes comparable to the gain-length, the 1D theoretical FEL model transitions from the Compton to the Raman limit [2]. In this work, we investigate the behavior of the FEL's gain-length and efficiency in these two limits. The starting point for the analysis was the one-dimensional FEL theory including space-charge forces. The derived results were compared to numerical results of Genesis 1.3 simulations. This theoretical model predicts that in the Raman limit, the gain-length scales as the beam current to the $-1/4^{\text{th}}$ power while the efficiency grows as the square root of the beam current.

INTRODUCTION

The attractiveness of sub-millimeter undulators is the ability to produce EUV and X-ray FELs in a compact space. A 100 MeV electron beam is easily obtainable in 10 meters with current acceleration technology and produces EUV light in an undulator of 800 μm period. A high-gain FEL requires beam currents in the kA scale in order to achieve saturation. The small aperture of such micro-undulators drives the transverse size of the beam to the 10 μm scale while their small undulator strength, $K_{und} \approx 0.01$, reduces the coupling of the beam and radiation. All these factors contribute to bring longitudinal space-charge effects to the foreground of compact FELs based on micro-undulators.

The typical FEL operation regime is the Compton regime, in which space charge is negligible. Marcus et al. [3] have shown that longitudinal space-charge increases the gain-length and provided a Ming Xie type of fit to the gain. However, if the longitudinal space-charge is strong enough, it can no longer be treated as only a correction to the Compton regime. Gover and Sprangle [2] treat the limit in which space-charge is dominant as a separate FEL regime. The transition into the Raman regime can be quantified as the set of undulator and beam parameters such that: $2k_p L_G > \pi$.

We will show that in the Raman limit, the gain-length and efficiency of the FEL change their scaling with the beam current from the typical scaling in the Compton regime. The gain-length tapers off to a $I_0^{-1/4}$ scaling at very high beam currents, while the efficiency is boosted to a $I_0^{1/2}$ scaling. The Raman limit presents a new mode of operation of the FEL. We investigate the behavior of gain and efficiency in the Raman limit. The analysis is carried out solely through the one-dimensional FEL theory in order to isolate the effects of longitudinal space-charge. To study FEL efficiency we begin by providing insight into the conditions for saturation. The 1D FEL theory yields analytic solutions for the gain, whose validity extends to the Compton and Raman limits. The efficiency is deduced by finding the saturation power that results for a given gain and saturation distance. The analytic expressions are then compared to simulations. A simple numerical approach was treated by a linear finite-difference numerical integration of the one-dimensional FEL equations with and without the space-charge terms. As a third consistency check, genesis 1.3 simulations were implemented. Since genesis 1.3 includes three-dimensional effects, the beam parameters for the simulated beams were chosen so as to minimize the effect of 3D space-charge, diffraction, and emittance.

1-D FEL THEORY

Longitudinal space charge is quantified by the relativistic plasma wave-number, and its effects on the FEL performance can be studied in the 1-D limit. The relativistic plasma wave-number is defined as:

$$k_p = \sqrt{\frac{2I_0}{I_A \gamma^3 \sigma_x^2}}$$

The Alfein current is, $I_A = 4\pi\epsilon_0 m_e c^3 / e$. The beam current, energy, and transverse size are I_0 , γ , σ_x , respectively. The transition into the Raman regime can be quantified as the set of undulator and beam parameters such that:

$$2k_p L_G > \pi$$

The gain-length is defined through the solutions of the third-order ODE for the electric field. Assuming the field has the form, $\vec{E}(z) \sim \exp(\alpha z)$, then the root with a positive real part defines the gain-length as:

$$\alpha^3 + i4k_u \alpha^2 + (k_p^2 - 4k_u^2 \eta^2) \alpha - i8k_u^3 \rho^3 = 0$$

$$\rightarrow L_G = \frac{1}{2\Re[\alpha_+]}$$

The undulator wavenumber is, k_u , the Pierce parameter is ρ , and the detuning from resonance is η . For completeness we quote the Pierce parameter:

$$\rho = \left[\frac{K[JJ] \gamma_z k_p}{4\sqrt{2} \gamma k_u} \right]^{2/3}$$

The following definitions are in order: k_u is the undulator wave-number, the peak magnetic field is B_u , so that the undulator parameter is $K = eB_u/mck_u$, and $[JJ]$ is a constant on the order of unity that describes the coupling between the electron motion and radiation.

Now we take the two limits in the cubic equation for the 1D FEL gain. In the Compton limit, the case with no space-charge, $k_p = 0$, we obtain the usual definition of the gain-length:

$$L_G^C = \frac{1}{2\sqrt{3}k_u\rho} \propto I_0^{-1/3}$$

When k_p can no longer be neglected in the cubic equation, the maximum gain is shifted to a detuning of, $\eta_{max} = k_p/2k_u$, and the gain-length's dependence on beam current shifts to:

$$L_G^R \propto I_0^{-1/4}$$

Efficiency of an FEL is defined as the power extracted from the electron beam. If the system's energy is to be conserved, the extracted beam energy has to be fed into the energy of the electromagnetic field. Therefore, we can write the following definition for FEL efficiency:

$$Q_{FEL} = \frac{\Delta U_{beam}}{U_{beam}} = \frac{\Delta P_{rad}}{P_{rad}} = \frac{e(P_{sat} - P_0)}{\gamma_0 mc^2 I_0}$$

Following the arguments presented in [2], we can derive the efficiency's dependence on the beam current for the two regimes:

$$Q_{eff}^C \propto I_0^{1/3}$$

$$Q_{eff}^R \propto I_0^{1/2}$$

To investigate these scaling rules through numerical methods, we take the saturation power to be the average power of the FEL after the exponential gain has subsided. This approach is useful in analysing simulations, but not analytically meaningful like the quasi non-linear methods implemented by Zhirong et al [4], [5] to study saturation. The topic of saturation power is a delicate one and is inherently a non-linear effect that is not the topic of this work.

NUMERICAL METHODS

A 1D solver was implemented to study the behavior of the FEL gain-length and saturation power as longitudinal space-charge effects become dominant. The coupled FEL equations [6] can be numerically integrated by a linear integration method as shown below.

$$\theta_j^n = \theta_j^{n-1} + 2k_u \eta_j^{n-1} \Delta z$$

$$\eta_j^n = \eta_j^{n-1} - \frac{e}{\gamma_0 mc^2} Re \left[\left(\frac{K[JJ]}{2\gamma_0} \tilde{E}^{n-1} - \frac{i\mu_0 c^2}{\omega_r} \tilde{J}_1^{n-1} \right) e^{i\theta_j^{n-1}} \right] \Delta z$$

$$\tilde{E}^n = \tilde{E}^{n-1} - \frac{\mu_0 c K[JJ]}{4\gamma_0} \tilde{J}_1^{n-1} \Delta z$$

$$\tilde{J}_1^n = j_0 \frac{2}{N} \sum_{j=1}^N \exp(-i\theta_j^{n-1})$$

$$j_0 = -\frac{ec}{\pi \sigma_x^2 \lambda_r} N$$

Space charge in these equations is strictly a longitudinal term and is proportional to the first harmonic of the electron bunching. Since the Raman limit arises in the one-dimensional FEL theory, it should manifest itself in the results obtained by “pushing” a particle distribution through the above equations. However, because the equations are general, they should also reproduce the Compton limit. Genesis 1.3 [7] is a 3D FEL code that is the standard in the community and we can use it to benchmark the 1D code and as a second point of comparison. In order to replicate the 1D condition in genesis, we must use pancake beams in which longitudinal space-charge is dominant. Care was also taken in preparing simulations that minimize the effects of diffraction and emittance.

GAIN AND DETUNING

Figure 1 shows the gain curves as functions of the detuning of the beam from resonance. The blue plot is made for a set of parameters that put the FEL in the Compton regime, but with enough space-charge for there to be detuning. The red plot is obtained for a set of parameters that drive the FEL into the Raman regime. There is good agreement between the analytic solutions, 1D model, and genesis1.3. The maximum gain (shortest gain-length) for a specific set of beam parameters is obtained for an energy detuning that depends on the space charge parameter, $\eta_{max} = k_p/2k_u$. The close agreement between the analytic solutions, the 1D model, and the genesis1.3 output for these two vastly different beam currents is encouraging and justifies our use of the 1D model.

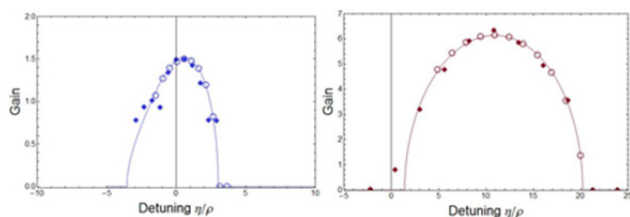


Figure 1: FEL gain as a function of the energy detuning of the electron beam. The solid line is the solution the cubic equation for the electric field, the circles correspond to 1D simulations, and the solid diamonds are genesis1.3 simulations. The left (blue) plot is an FEL in the Compton limit and the right (red) is the Raman limit.

LONGITUDINAL PHASE-SPACE

Figure 2 shows snapshots of the longitudinal phase-space of the electrons close to saturation of the high-gain FEL in the Compton (blue) and Raman (red) limits. We see that as the FEL approaches the point of saturation, the electrons lose energy and reach the bottom of their synchrotron oscillation inside the pondermotive bucket. In the Compton case, the particles continue to spin around the center of the bucket as a whole. However, in the Raman case, there is a point of charge pile-up that causes particles to significantly accelerate and alter their trajectories inside the bucket [8]. This prevents the synchrotron oscillations to continue undisturbed through saturation and smears out the energy distribution. The inclusion of longitudinal space-charge disturbs the synchrotron oscillations. In the simulations without space-charge the energy has a better defined oscillation that corresponds to the synchrotron frequency. Once space-charge effects are included, the average energy after saturation does not execute a well-defined oscillation.

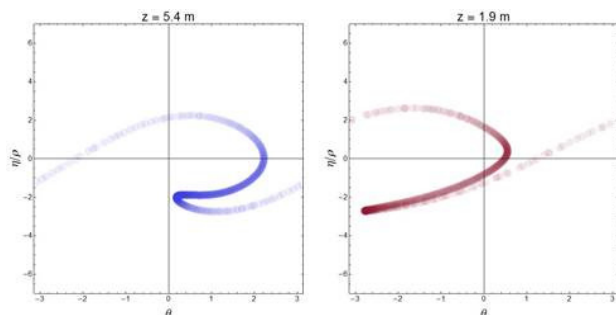


Figure 2: The longitudinal phase-space at the onset of saturation for the Compton (left and blue) and Raman (right and red) limits.

GAIN-LENGTH AND EFFICIENCY

The final two plots show the scaling of the gain-length and efficiency through the Compton and Raman regions of operation. To obtain these plots, we transition the FEL by varying the beam current while holding the rest of the set of undulator and beam parameters constant. Increasing the beam current indefinitely is not practical, but serves as

the most straightforward way to study the Compton-Raman transition and the FEL's performance there. The current directly increases the space charge's influence and, as seen above, changes the required detuning for maximum gain. The plot has Ln-Ln axes so that the slope of the lines corresponds to the power of the current dependence, $L_G \propto I_0^\alpha \rightarrow \ln(L_G) \propto \alpha \cdot \ln(I_0)$. The two sets of beam parameters for which we bench-marked our code with genesis are included (diamonds), and they show complete agreement with our 1D code (solid circles) and the asymptotic analytic behavior (solid lines).

Figure 3 confirms the scaling law for the FEL gain-length for a wide range of beam current values (1kA to 1.6MA). For low beam currents, the gain-length shortens as $I_0^{-1/3}$ for an increase in current. Although there is detuning and space charge is not negligible in this region, this is still the Compton limit. As the beam current is increased, the plasma wave-length approaches a gain-length and begins to strongly influence micro-bunching. This increases the gain-length and an increase in current no longer translates in as much of a shortening of the gain-length as in the Compton limit. In fact, in the Raman regime, the gain-length is proportional to, $I_0^{-1/4}$.

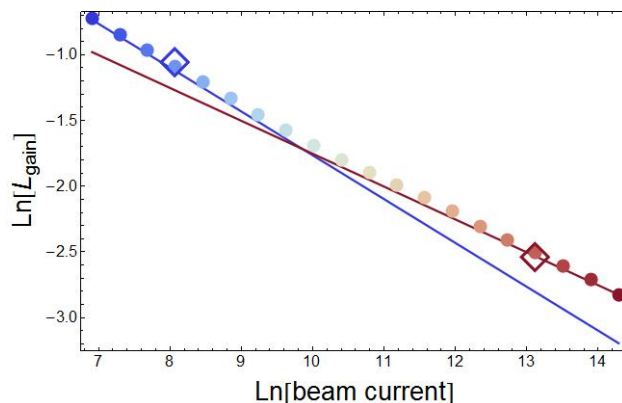


Figure 3: Gain-length scaling with beam current. Blue is the Compton limit and red Raman.

Although the gain-length increases for as more current is added, the efficiency of the FEL process begins to increase. Gover and Sprangle [2] derive the efficiency in the Raman limit to be proportional to the plasma wave-number, which in turn depends on the square root of the beam current, $Q_{eff}^R \propto k_p \propto I_0^{1/2}$. The efficiency boost stems from the large detuning needed for the space charge dominated FELs. Because the electrons are higher off resonance initially, once saturation occurs and the particle distribution has reached the bottom of its synchrotron oscillation in the pondermotive bucket, there has been more energy lost to the radiation as compared to a slightly detuned beam. Figure 4 confirms the efficiency increases from, $Q_{eff}^C \propto I_0^{1/3}$, to $Q_{eff}^R \propto I_0^{1/2}$, as the FEL transitions from the Compton to the Raman regime.

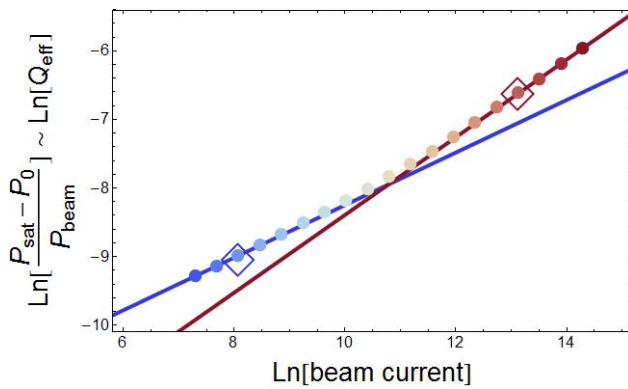


Figure 4: Efficiency scaling with beam current. Blue is the Compton limit and red Raman.

DISCUSSION

Space charge effects in high-gain FELs are usually a corrective term that increases the ideal gain-length and postpones saturation. We have studied the extreme case of a Raman FEL, where longitudinal space charge is dominant. Once in the Raman limit, there is a trade-off between the gain-length and efficiency of the FEL. We have confirmed through simulations that while the gain-length tapers off to a $I_0^{-1/4}$ scaling at very high beam currents, the efficiency of the FEL is boosted to a $I_0^{1/2}$ scaling. The onset of saturation has been shown to be affected by the space dynamics as shown in the longitudinal phase-space plots.

The push towards sub-millimeter period undulators for the construction of compact XFELs requires electron beams that have high current and small transverse size at energies of hundreds of MeV. These micro-undulators have small undulator parameters, $K_{und} \approx 0.01$, which further decreases the coupling of the beam and radiation. It is not unreasonable to expect that Raman effects will surface in such scenarios.

REFERENCES

- [1] J. Harrison, A. Joshi, J. Lake, R. Candler, and P. Musumeci, "Surface-micromachined magnetic undulator with period length between 10 μm and 1 mm for advanced light sources," *Phys. Rev. Spec. Top. - Accel. Beams*, vol. 15, no. 7, p. 070703, Jul. 2012.
- [2] A. Gover and P. Sprangle, "A Unified Theory of Magnetic Electrostatic Bremsstrahlung Scattering, and Cerenkov-," *IEEE J. Quantum Electron.*, vol. QE-17, no. July, pp. 1196–1215, 1981.
- [3] G. Marcus, E. Hemsing, and J. Rosenzweig, "Gain length fitting formula for free-electron lasers with strong space-charge effects," *Phys. Rev. Spec. Top. - Accel. Beams*, vol. 14, no. 8, p. 080702, Aug. 2011.
- [4] Z. Huang and K.-J. Kim, "Review of x-ray free-electron laser theory," *Phys. Rev. Spec. Top. - Accel. Beams*, vol. 10, no. 3, p. 034801, Mar. 2007.
- [5] N. Vinokurov, Z. Huang, O. Shevchenko, and K.-J. Kim, "Quasilinear theory of high-gain FEL saturation," *Nucl. Instruments Methods Phys. Res. Sect. A Accel. Spectrometers, Detect. Assoc. Equip.*, vol. 475, no. 1–3, pp. 74–78, Dec. 2001.
- [6] P. Schmüser, *Springer Tracts in Modern Physics 258 Free-Electron Lasers in the Ultraviolet and X-Ray Regime*.
- [7] S. Reiche, "Numerical Studies for a Single Pass High Gain Free-Electron Laser Dissertation," 1999.
- [8] E. Peter, a. Endler, F. B. Rizzato, and a. Serbeto, "Mixing and space-charge effects in free-electron lasers," *Phys. Plasmas*, vol. 20, no. 12, p. 123104, 2013.